POROSITY AND REDUCIBILITY OF EXTRUSION BRIQUETTES

Aitber Bizhanov[1], Bhagiratha Mishra[2]

1) J.C.Steele&Sons, Inc., Representative in Russia&CIS, Turkey
2) Dalmia Institute of Scientific & Industrial Research, Rajgangpur, India

Abstract:

Porosity of the briquettes made by Stiff Vacuum Extrusion (extrusion briquettes) has been investigated by the combination of the Scanning Electronic Microscopy (SEM) and X-ray computed tomography with the help of the STIMAN procedure. The values of the porosity are comparable with (or better) than the typical values for the alternatively agglomerated products (indurated pellets, traditional briquettes). Two types of extrusion briquettes were investigated: for BF and for solid-state reactors. All these briquettes are being used industrially or underwent the full-scale trials as the charge components of the industrial furnaces. Reducibility of these extruded briquettes is influenced by the porosity and the mineralogy of the briquette's component's phases during reduction. The briquettes made of the LD sludge and BF flue dust with the addition of the iron ore fines are studied in comparison to the lumpy iron ore from the same deposit. Under the considered experimental conditions extrusion briquettes exhibited better reducibility, which can be attributed to the presence of carbon in the BF dust and to the ferrites. Silicates represent bonding melt in iron ore. Briquettes for solid-state reduction bonded with the magnesium based binder show very high metallization levels.

KEY WORDS: extrusion briquette; stiff vacuum extrusion; Blast Furnace, solid-state reactor, Coke rate, hot strength.

INTRODUCTION

Agglomeration of the fine natural and anthropogenic substances of the iron and steel making attracts permanent attention. In the present study we consider the briquetting technology based on the stiff vacuum extrusion [1-2)] as the prospective routine to process such materials. This approach helps to take the advantage of a good green mechanical strength of the extrusion briquettes [3)] and of their approved high metallurgical properties[4)] including high hot strength.

Present paper is devoted to the research of the porosity and the reducibility of the extrusion briquettes.

We have selected two different types of the extrusion briquettes: for BF and for solid-state reactors.

1. POROSITY OF THE EXTRUSION BRIQUETTES FOR BLAST FURNACE

For the metallurgical processes with the gaseous reducing agent the porosity of the charge components plays essential role. Increase in porosity values (within certain boundaries) generally leads to better reducibility of the agglomerated charge components.

To investigate the porosity of the extrusion briquettes we have applied the Scanning Electronic Microscope LEO 1450 VP (Carl Zeiss, Germany) with the resolution 3.5 nm together with the X-ray high-resolution computed tomography system Phoenix V|tome|X S 240 (General Electric, USA). X-ray computed tomography has been used to detect the share of the macro pores (size larger than 100 μ m). For the smaller size pores the SEM had been applied. The

approach based on the STIMAN[5)] computer software has been used to calculate the porosity and to investigate the structure and morphology of the pores. Apparent porosity was also measured according to DIN 51056.

Briquettes for BF extrusion briquettes have the following composition: 47.2% LD sludge, 28.3% flue dust, 18.9% iron ore fines, 4.7% Portland cement and 0.9% Bentonite.

Mineralogical composition of the extrusion briquettes components is as follows from Table 1. Worth to mention is that the BF dust (or flue dust) contains calcium ferrite (Fig. 1). Together with the well-known presence of the carbon in the flue dust this plays essential role in the reduction of the briquette.

Table 1 Phase composition of the extrusion briquettes components

	Major phases	**Minor phases**
Iron ore fine	Hematite	Goethite, Gibbsite, Kaolin, Pyroxene
BF dust	Magnetite, Hematite, Graphite	Wustite, quartz, Calcium ferrite
LD sludge	Magnetite, Wustite	Wollastonite, calcite
EAF dust	Magnetite, Wustite,	Calcite, Wollastonite, Zinc oxide, Lead oxide Graphite

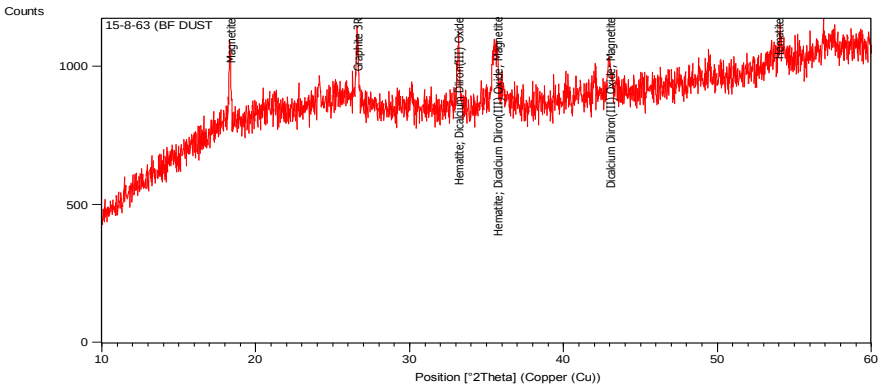

Visible	**Ref. Code**	**Score**	**Compound Name**	**Displace-ment [°2Th.]**	**Scale Factor**	**Chemical Formula**
*	98-001-7170	40	Graphite 3R	0.000	0.887	C1
*	98-010-6386	40	Hematite	0.000	0.805	Fe2 O3
*	98-005-4400	7	Dicalcium Diiron(III) Oxide	0.000	0.479	Ca2 Fe2 O5

Figure 1 X-ray Diffractogram of BF dust shoeing the presence of Dicalcium Diiron (III) oxide

Table 2 gives the chemical compositions of the briquette components.

Table 2 Chemical composition of the substances

Elements	Iron ore fines	BF dust	LD sludge
Fe_2O_3/ FeO	78.5	51.5	87.5
SiO_2	5.6	6.3	0.6
CaO	-	4.9	9.5
MgO	-	0.2	1.2
Al_2O_3	5.4	5.1	0.3
TiO_2	0.8	-	-
C		30.5	-
Fe_{total}	53.5	35.6	64

Typical chemical analysis of the iron ore and the extrusion briquettes components is given in Table 3.

Table 3 Chemical analysis of the iron ore and extrusion briquettes

CA (wt. %)	Iron ore	Briquette
CaO	0.2	7.4
SiO2	2.21	4.6
Al2O3	3.11	4.35
Fe2O3	88.53	68.03
MgO	-	0.4
K2O+Na2O	0.2	0.2
TiO2	0.22	0.23
LOI	5.82	15.02

We have measured physical properties of the extrusion briquettes in their strengthening evolution (from green to cured after one week). These values are given in Table 4. It follows from measurement that the porosity of the extrusion briquettes is comparable with the porosity of the indurated pellets and is larger than the porosity of the majority of the iron ores.

Porosity and cold compressive strength curves are shown at Fig. 2. One can see the existence of the strength and porosity local maximum on the day 3. This phenomenon was explained by Bizhanov[4)] as being related with the creation of the Bentonite induced coagulation structure which finally is substituted by the Portland cement hydration.

Table 4 Physical properties of the BF briquettes.

Curing	AP%	Bulk density (gm/cc)	CCS (kg/cm^2)
Green	31.5	2.42	24
1 day	25.4	2.66	45

2 days	32	2.43	63
3 days	27	2.44	52
4 days	27.2	2.45	56
5 days	26.2	2.45	57
6 days	26.8	2.46	59

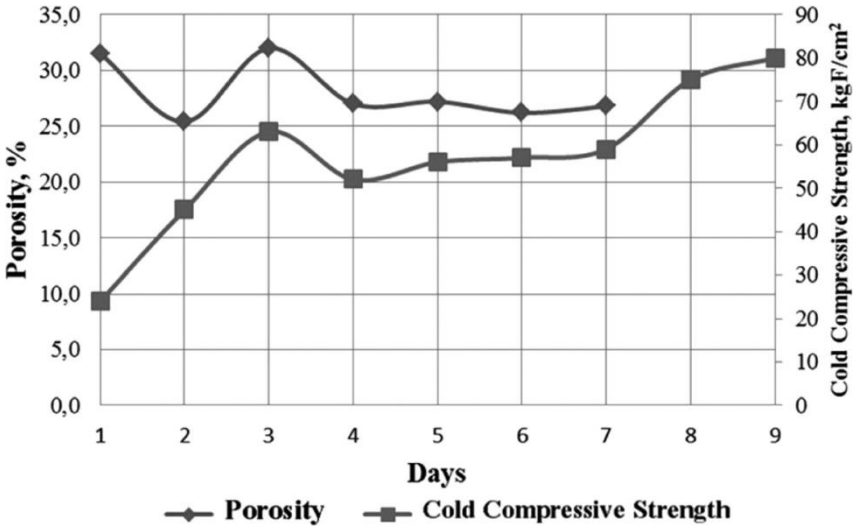

Figure 2 Porosity and cold compressive strength values during the strengthening of BF briquettes

The values of the porosity appeared to match with those calculated by SEM+X-ray computed tomography procedures. Figure 3 shows the tomographic image of the distribution of the pores with the sizes larger than 100 μm in the briquette body.

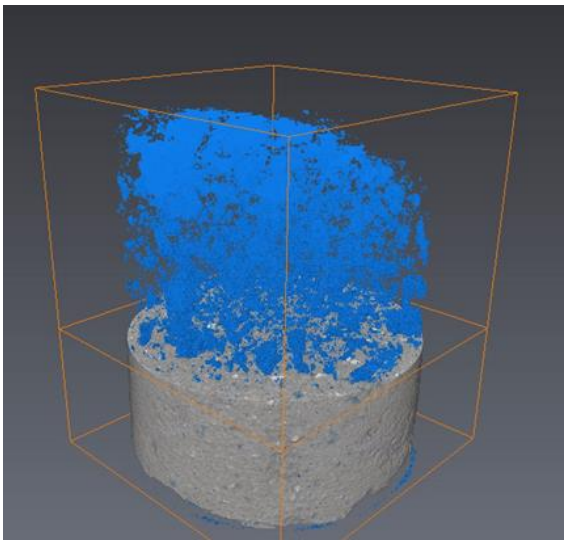

Figure 3 Distribution of the pores with the sizes larger than 100 μm

2. REDUCIBILITY OF THE EXTRUSION BRIQUETTES FOR BLAST FURNACE

Comparative reducibility test for iron ore and extrusion briquettes was done in a control atmosphere furnace connected with vacuum pump and constant air supply with regulator. A hollow alumina tube having length 1000mm, outside diameter 85 mm and inside diameter 75mm makes the test chamber. Weights of the extrusion briquettes and iron ore are taken before and after incipient fusion at 1300°C for 30 minutes. Extrusion briquettes and iron ore are placed in graphite crucible inside alumina crucible covered by coke breeze having size 1-5mm throughout the diameter engulfing the graphite crucible completely. Thickness of the coke layer is 25mm. Then it was blocked by perforated plug from both sides and covered by insulating blocks. Water-cooled metallic clamps were fitted in both the side of alumina tube. Vacuum pump is connected in one of the clamp along with air supply connected with flow meter. Before staring the heating, the inside chamber of the alumina tube was evacuated up to 0.5mbar. The furnace was started with a heating rate of 10°C/Min. When the furnace attained 800°C air supply was started at a rate of 10 liters/min till the completion of the test. Both extrusion briquettes and iron ore are fired from 1000°C to 1500°C for 2 hours in step of 100°C.

Reducibility was determined from oxygen loss calculated from weight. Metallic iron content and metallization was evaluated. Reducibility, metallic iron content and metallization of iron ore and extrusion briquettes are given in Table 5.

Table 5 Metallization and reducibility of iron ore/extrusion briquettes

T, °C	**$Fe_{metallic}$, %**	**Fe_{total}, %**	**Metalization %**	**Reducibility %**
1000	2.16/14.20	67.48/60.5	3.20/23.5	35/48
1100	12.69/20.96	69.52/61.7	18.25/33.97	52/62
1200	17.65/30.36	70.25/63.7	25.10/47.6	61/72
1300	30.33/44.74	73.3/65.6	41.30/68.2	65/80
1400	53.75/47.04	80.79/67.46	66.53/69.7	82/88
1500	84.25/79.22	90.4/80.87	93.20/97.95	93/99

Phase analysis of iron ore fired at different temperature is given in Table 6.

Table 6 Major and minor phases in iron ore and extrusion briquettes at different temperatures

	Iron ore		**Extrusion briquettes**	
T, °C	**Major phase**	**Minor Phase**	**Major phase**	**Minor Phase**
As such	Hematite	Goethite	Hematite, Magnetite, Maghemite	Calcite
1000	Hematite, Magnetite, Wustite	Almandine	Iron, Magnetite, Hematite	Wustite, Hedenbergite, Akermanite-gehlenite
1100	Magnetite, Wustite	Almandine, Ferrous	Iron, Wustite, Magnetite	Stebrodolskite, Mellilite

1200	Magnetite	Wustite, Iron, Almandine	Iron	Magnetite, Calcium ferrite, Akermanite-Gehlenite
1300	Magnetite, Wustite	Iron, Iscorite, Almandine	Iron	Wustite, Hedenbergite, Glass
1400	Iron	Wustite, Glass	Iron	Wustite, Glass
1500	Iron	Glass	Iron	Glass

We have also estimated the dynamics of the values of the physical properties of the extrusion briquettes while firing at different temperatures (for the non-cured samples). These values are given in Table 7 in comparison with the values of the physical properties of the iron ore and indurated pellets.

Table 7 Porosity and reducibility after firing Extrusion briquettes at different temperature in comparison with iron ore and indurated pellets

Briquette/ Lumpy iron ore/ Indurated pellet	**Apparent porosity %**	**Bulk density (gm/cc)**	**Reducibility%**
Green	25.8/18.4/36.2	2.60/4.11	-
500°C	33.66/19.4	2.674.04	-
1000°C	37.36/29.15	2.81/3.63	48/35
1100°C	37.28/27.6	2.61/3.84	62/52
1200°C	46.87/24.5/27	2.56/3.92	72/61
1300°C	29.71/21.3	3.08	80/65
1400°C	22.6	3.19	88/82

Microscopic evaluation of iron ore and pellets fired at different temperature are evaluated on polished section under reflected light in a universal microscope with image analyzer. Photomicrograph of iron ore fired at 1100°C and 1400^{o}C are given in Fig. 4-5. Photomicrograph of briquettes fired at 1100°C and 1400^{o}C are given in Fig. 6-7.

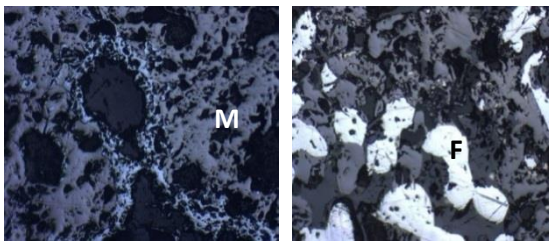

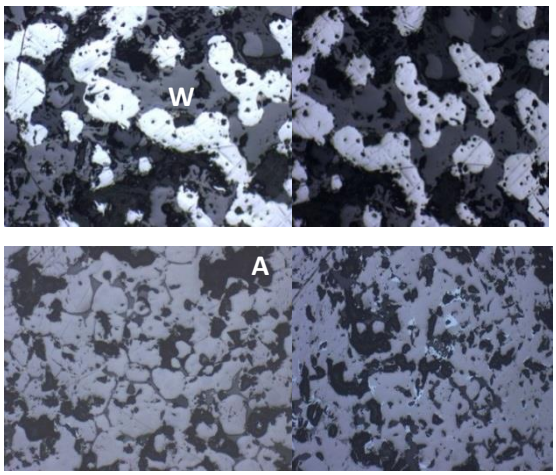

Figure 4 Iron ore fired at 1100^{o}C Magnetite (M); Wustite (W); Iron (I); Almandine (A).

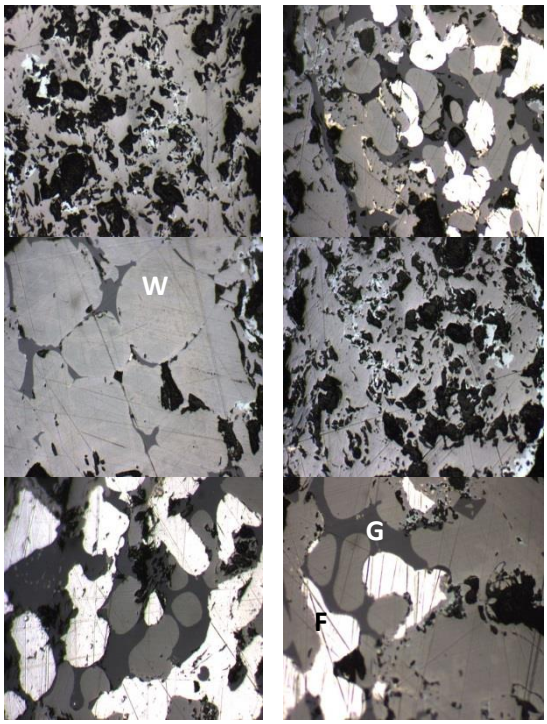

Figure 5 Iron ore fired at 1400^{o}C Wustite (W); Iron (I); Glass (G).

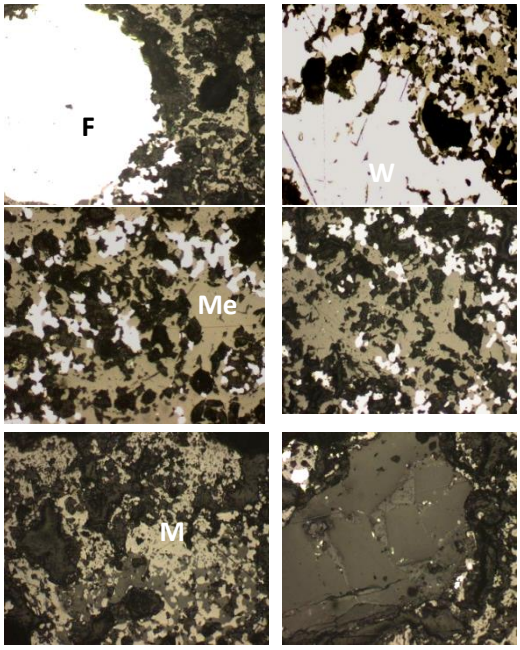

Figure 6 Briquette fired at 1100^{o}C Magnetite (M); Wustite (W); Iron (I); Mellilite (Me).

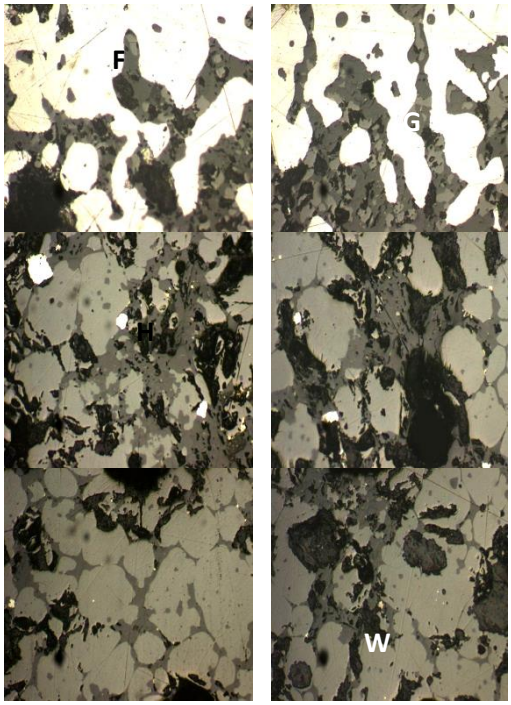

Figure 7 Briquette fired at 1300^{o}C Wustite (W); Iron (I); Glass G).

It follows from the chemical, phase and mineralogical analysis that the degree of reducibility is higher in case of extrusion briquettes than for iron ore samples.

Under the particular conditions of the applied test facility better reducibility of extrusion briquettes can be explained by principally different mineralogical structure of the agglomerated product and of the iron ore at different temperatures. Major silicate phases after firing of iron ore samples at different temperature is iron silicate and iron aluminium silicate which might envelope the iron ore grains and thus retard the reduction. In case of extrusion briquettes presence or formation of ferrite which is easier to reduce than iron silicate or iron aluminium silicate may have facilitated the reduction[6]. Ferrite was brought to the extrusion briquettes by flue dust or might have been additionally generated at the presence of calcium oxides due to the very high basicity of extrusion briquettes[7-10]. The latter looks possible since the conditions in the applied test facility partially simulate the sintering process (burning Coke) where the ferrites are very well known to appear. Another evident reason for better reducibility of the extrusion briquettes follow from the mentioned above presence of the carbon in the flue dust (up to 25%). Closer contacts of the carbon and oxides particles facilitate the reduction.

3. POROSITY AND REDUCIBILITY OF THE EXTRUSION BRIQUETTES FOR SOLID-STATE REDUCTION

Table 8 shows the compositions of the extrusion briquettes we have chosen for the utilization as the charge components for the direct solid-state reduction in the industrial reactors.

Table 8 Extrusion briquettes compositions for the solid-state reduction

Briquette components	**01-01**	**01-02**	**01-03**
Pellets fines	50,0	50,0	50,0
Sludge	25.0	25,0	25,0
Mill scale	15,0	15,0	15,0
EAF dust	5,0	4,75	5,0
Slaked lime	5,0		
Portland cement		5,0	
Magnesium binder			5,0
Bentonite		0,25	

Morphological microstructure investigation has been conducted using the regime of secondary electrons, which allows obtaining high-quality halftone images in a wide range of magnifications. The STIMAN procedure allows obtaining correct images with clear boundaries between the pores and particles. Quantitative analysis of microstructure was carried out using the software "STIMAN" by two methods. 1 – based on a set of SEM-mode images in the regime of the reflected electrons, 2 – complex analysis of the set of SEM images and X-ray computed tomography with various amplifications.

Measured in this way the morphological parameters of the extrusion briquettes and pore characteristics are listed in table 9. The values of the apparent porosities measured by DIN 51056 were at the level of 24.5% for the cured briquettes and 33.5% after reduction.

It follows from these data that the largest growth in the porosity values after reduction exhibited the briquette bonded by a magnesium based binder (under Patenting) – 19.5% against 13% for the lime bonded one and only 2.6% for the Portland cement bonded briquette. The reasons for this are related with the specifics of the mineralogical structures of these briquettes during their reduction and with their different mechanical strengths. The harder the briquette is mechanically to smaller extent it will be subjected to the pores generation due to the volume changes conjugated with the Hematite-Magnetite phase transitions. The smaller the gain in porosity the smaller the reducibility rate is.

Table 9 Porosity and pores micromorphology measured by SEM (STIMAN)+X-ray tomography

Sample	**Porosity SEM/SEM + X-ray tomography**	**Sizes distribution ($n_{из}$), %**					Maximum diameter	Shape factor		
	n, %	D_1	D_2	D_3	D_4	D_5	Dmax	K_f		
		<0.1*	0.1-1.0	1.0-10	10-100	>100				
01-01	31,6	0,6	8,6	25,6	65,2	0,0	57,6	0,25 - 0,33	0,42 - 0,50	
	37,3	0,5	7,2	21,4	66,8	4,1	407,2			
01-01-reduced	32,9	0,2	9,0	38,4	52,4	0,0	70,94	0,25 - 0,33	0,42 - 0,50	0,75 - 0,83
	38,3	0,1	7,7	32,4	49,8	10,0	504,49			
01-02	31,2	0,6	8,0	30,1	61,3	0,0	45,78	0,33 - 0,42		
	35,7	0,5	7,0	26,2	61,3	5,0	299,96			
01-02-reduced	37,9	0,2	9,3	31,1	59,1	0,3	100,51	0,33 - 0,42	0,50 - 0,58	
	40,4	0,2	8,9	29,5	55,2	6,2	583,77			
01-03	31,8	0,6	5,8	28,4	65,2	0,0	62,92	0,42 - 0,50		
	32,9	0,5	5,5	27,2	65,3	1,5	191,89			
01-03-reduced	32,8	0,2	3,2	35,7	60,9	0,0	71,75	0,42 - 0,50	0,58 - 0,67	0,75 - 0,83
	39,3	0,2	2,6	28,9	58,0	10,3	736,41			

*- in μm

1. n – total porosity calculated by SEM image.
2. D_1, D_2, D3, D_4, D_5 – different dimension categories of pores.
3. D_{max} – maximum pore diameter.
4. K_f – pore shape factor. Calculated as the ratio of small and large semi-axes of the ellipse inscribed in pore. For isometric pores K_f=0.66-1.00, for anisometric - K_f=0.1-0.66, for the hole-type Kf<0.1.

Fig. 8 shows the difference in the pore structure and distribution for the considered briquettes. These are SEM images processed by the STIMAN procedure.

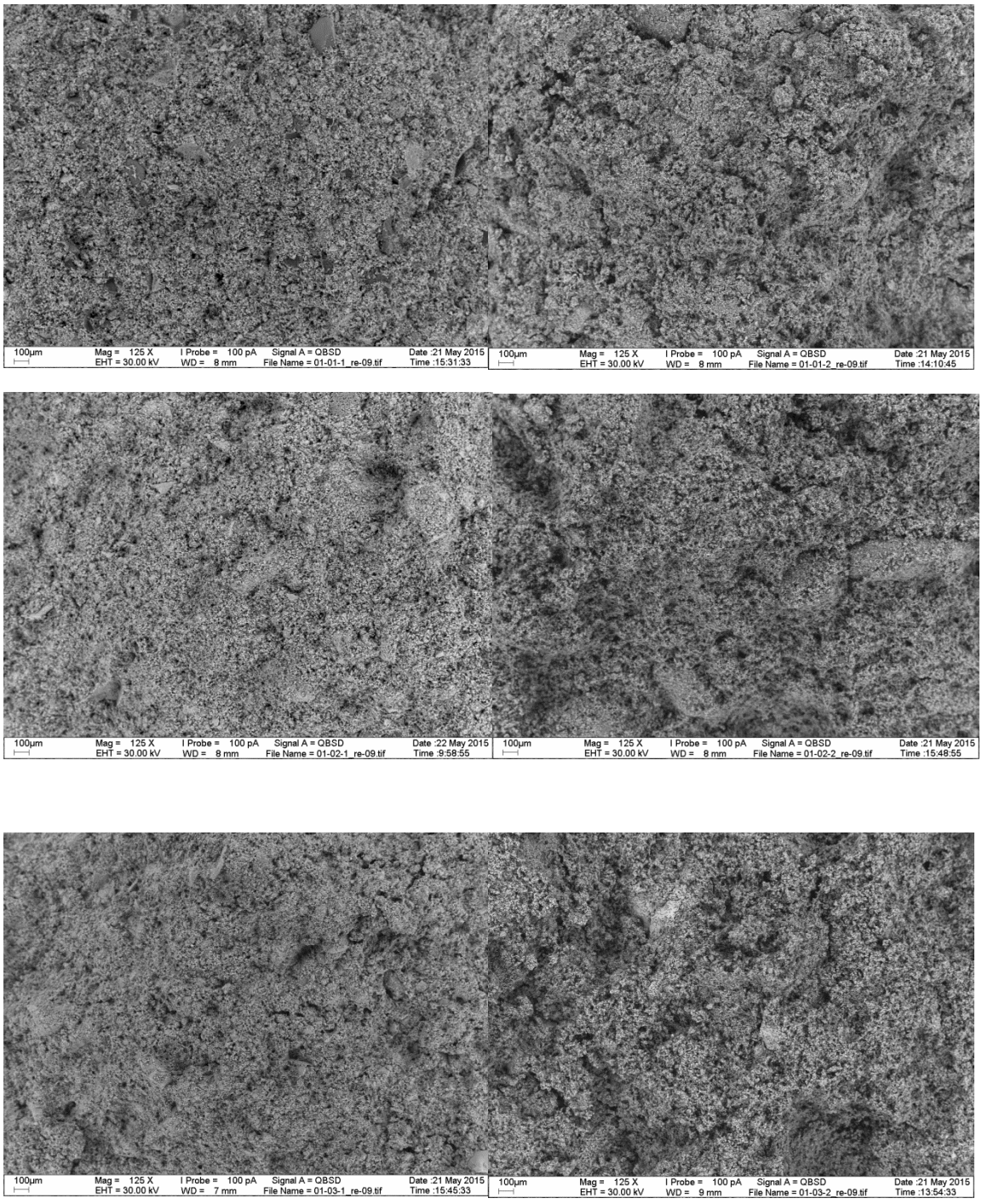

Fig. 8 Comparison of the pores distribution in the cured and reduced extrusion briquettes (top row – briquette 01-01, lime bonded; middle row – 01-02, cement bonded; bottom row – 01-03, magnesium based binder)

The values of the metallization and iron contents (total and metallic) of these briquettes are given in Table 10. Of all these briquettes only the sample 01-03 (magnesium based binder) can be considered as adequate candidate for the industrial utilization in the direct reduced iron production reactors.

Table 10 Metallization and iron contents of the reduced extrusion briquettes.

Elements and oxides	**01-01**	**01-02**	**01-03**
Fe_t	74,86	69,02	86,86
Fe_{met}	49,11	18,66	84
Metallization,%	65,6	26,96	96,71

CONCLUSIONS

Porosity of the extrusion briquettes at different temperatures is comparable or better than the known values of the porosity of the indurated pellets. Extrusion briquettes made of the LD sludge and BF flue dust with the addition of the iron ore fines exhibited better reducibility than the lumpy iron ore of the same deposit. Better reducibility may be related with difference in mineralogical evolution of the extrusion briquettes and iron ore during reduction. The essential role in better reducibility of the extrusion briquettes belongs to the ferrites which are known to exhibit better reducibility. Presence of the carbon in BF dust also contributes to their better reducibility.

Extrusion briquettes bonded by a new magnesium based binder can be used as the charge component for the solid-state reduction processes.

REFERENCES

1) Y. K. Dalmia, I. F. Kurunov, R. B. Steele and A. M. Bizhanov: Metallurgist, (2012), No. 3, 39.
2) A. M. Bizhanov, I. F. Kurunov et al. Metallurgist. 56 (2012), 489.
3) I.F.Kurunov, A.M.Bizhanov, D.N.Tikhonov, N.R.Mansurova: Metallurgist. (2012), No.6, 44.
4) A.Bizhanov,I.Kurunov, Y.Dalmia, B.Mishra, S.Mishra: ISIJ Int., 55 (2015), No. 1, 175.
5) Sokolov V.N., Yurkovets D.I., Melnik V.N., Boyde A., Howell P.G.T. 3D reconstruction of surface and subsurface structures of solids by SEM stereo images. Inst. Phys. Conf. Ser. № 168: Section 4. Electron Microscopy and Analysis 2001. Proc. Of the Institute of Physics Electron Microscopy and Analysis Group Conference, University of Dundee, 5-7 September 2001. Institute of Physics Publishing. Bristol and Philadelphia, p. 119-122.
6) L.v.Bogdandy, H.-J.Engell: The reduction of iron ores. Sringer-Stahleisen, 1971.
7) W.A.Knepper, R.B.Snow, R.T.Johnson: Study of the Properties of Self-Fluxing Sinters, Agglomeration, Interscience Publishers, New York, (1962), p.787-804
8) D.A.Kissin, T.I.Litvinova: Mechanism of Mineral Formation in Sintering Fluxed Sinter, Stal (in English), (1960), No. 5, p.318-323
9) P.F. Nogueira, R.J. Fruehan: *Metallurgical and Materials Transactions B*, 2004, 35 B, 829
10) P.Kaushik, R.J.Fruehan: *Ironmaking & Steelmaking* 2006, 33, No. 6, 507-519